

# **IMPROVED MEASUREMENTS OF EXTERNAL HEAT RATES ON LAUNCH VEHICLES**

**Thomas R. Reinarts**

Launch Services Program Office, NASA Kennedy Space Center

## **ABSTRACT**

Knowledge of aerothermally induced convective heat transfer and plume induced radiative heat transfer loads is essential to the design of thermal protection systems for launch vehicles. Typically, Schmidt-Boelter gauges, taking advantage of the 1-D Fourier's law, measure the incident heat flux. This instrumentation, when surrounded by low-conductivity insulation, has an exposed surface temperature significantly lower than the insulation. As a result of this substantial disturbance to the thermal boundary layer, the heat flux incident on the gauge tends to be considerably higher (potentially by factors of 2 or more) than it would have been on the insulation had the calorimeter not been there. In addition, the gauge can receive energy radially from the hotter insulation, contributing to the increase of the indicated heat flux. This paper will present an overview of an effort to account for these effects and improve the accuracy of such measurements. Model calibration testing performed on flat plates exposed to an aerothermal environment will also be discussed, as will alternate heat flux measurement techniques.

## **INTRODUCTION**

An instrument placed into a system to measure a given effect changes the environment simply by its addition to the system. Therefore, the measured value deviates by some amount from the undisturbed value, and it is important to understand the magnitude of this deviation. The deviation is small for many types of measurements, but can be substantial for heat flux gauges on launch vehicles. Since analytical models used to predict heat flux loads on launch vehicles are frequently calibrated by in-flight measurements from heat flux gauges, it is important to understand the contributing factors to sensor disturbance of the environment and its impact on sensor measurements. In areas with TPS, the dominating contributor is the potentially large temperature difference between the hotter, low conductivity insulation and the adjacent cooler gauge. This results in an incident heat flux indicated by the gauge that is higher than it would be on the insulation if the gauge had not been introduced into the system, potentially by factors of two or more. There are two causes of this (Figure 1). First, the near step change in wall temperature from TPS to sensor disturbs the thermal boundary layer, producing a higher incident flux on the sensor<sup>1,2</sup>. Second, the lower temperature gauge also acts as a heat sink, causing a radial flow of energy through the sides of the gauge that moves through the epoxy/wafer/thermopile and down the gauge body, which increases the indication of surface normal incident heat flux.

An effort to quantify these effects for a Schmidt-Boelter heat flux sensor (by far the most common heat flux sensor used on launch vehicles) has been undertaken in a three-part study, which includes modeling of the external velocity and temperature boundary layers, modeling of

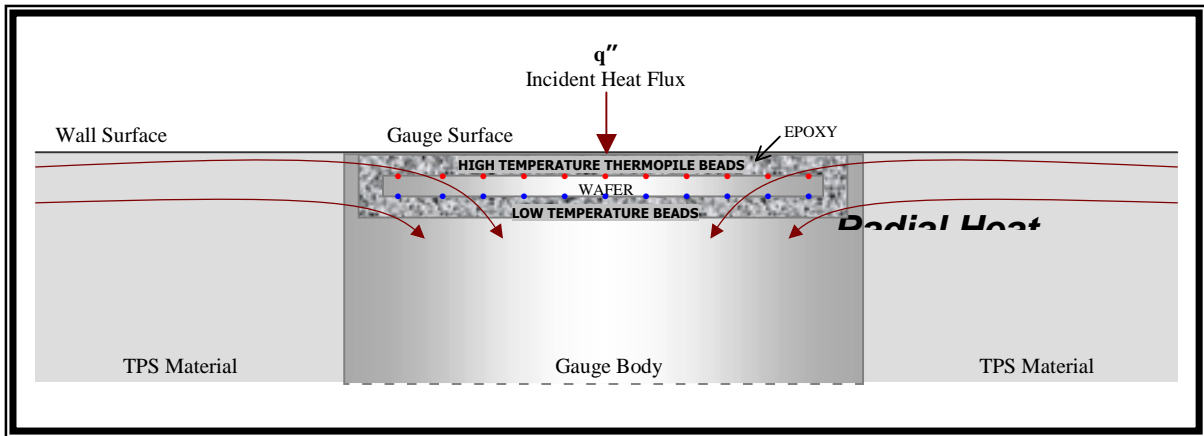


**Figure 1: Diagram of Heat Transfer through a Schmidt-Boelter Gauge**

the conductive heat transfer within the sensor and from the surrounding TPS to the sensor, and testing in an aerothermal facility at Marshall Space Flight Center (MSFC). The overall modeling and calibration effort will eventually be used to quantify and correct the in-flight sensor errors. The expected result is an improved understanding of aerothermally induced convective heat transfer on launch vehicles, reduced design loads, and relaxed TPS requirements. While current data provide conservative factors of safety, there are potential benefits attainable from reduced conservatism via lower TPS mass and reduced TPS application requirements. An alternative method for heat flux measurement is also explored. This includes measuring the time rate of change of the surface temperature and inferring an incident heat flux from that data.

## BOUNDARY LAYER ANALYSIS

In convective flow, dramatic thermal boundary layer changes can result from steep surface thermal gradients in the direction of flow. The heat transfer from a convective flow to the plate can be described by the following equation:

$$(1) \quad q'' = -k_f \nabla T_{f0}$$

where  $k_f$  is the thermal conductivity of the fluid,  $T_{f0}$  is the temperature of the fluid,  $\nabla$  is the gradient operator, and  $q''$  is the fluid/wall heat-flux.

Thus, a dramatic change in wall surface temperature results in a change in the fluid thermal gradient at the wall interface, causing a changed heat flux into the wall. Schmidt-Boelter gauges are typically made of materials with relatively high specific heat and high thermal conductivity. When surrounded by a TPS with low conductivity, the surface temperature gradient from TPS to gauge can be steep. In this situation, the heat flux into the gauge is not the same as the heat flux into the same area if the gauge is not present. Attempts at modeling this phenomena have been made<sup>1,2</sup>. These models assumed a step change in wall temperature, and constant fluid properties over the

surface temperature gradients. A CFD effort has been undertaken to include fluid property variations and calculate the difference between the gauge incident and undisturbed heat fluxes.

Referencing Figure 1, the magnitude of this dissimilar material effect is dependent on fluid properties, flow conditions at the leading edge, flow development length, calorimeter size, and of course the surface temperature gradient.

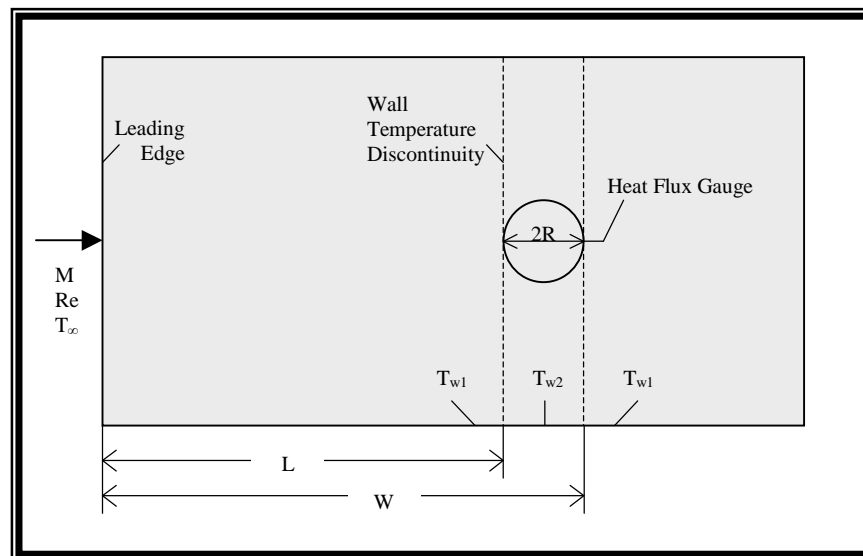


Figure 2: Diagram of CFD 2-D Plate Model

## CONDUCTIVE HEAT TRANSFER ANALYSIS

In addition to boundary layer effects, hotter surrounding TPS can conduct energy into the calorimeter and cause the calorimeter to indicate a higher than actual surface incident heat flux. To understand the conductive heat transfer effects on a Schmidt-Boelter gauge, it is important to also understand the operation and construction of the gauge. The Schmidt-Boelter gauge includes a coiling of thermopile wire around a wafer, which is encased by a low conductivity epoxy. The thermopile beads are located on the top (high temperature thermopile) and bottom (low temperature thermopile) of the wafer surface. These thermopile beads provide a temperature gradient that, based on appropriate calibration and the one-dimensional Fourier's law of heat conduction (Equation 2), outputs the incident heat flux.

$$(2) \quad q'' \propto \frac{\delta T}{\delta x}$$

Fourier states that, for steady state one-dimensional heat transfer through a given material, the heat flux,  $q''$ , is directly proportional to the differential temperature,  $\delta T$ , divided by the differential length,  $\delta x$ . Since the gauge's operation is based on this temperature difference between the upper and lower surface of the wafer, the radial heat transfer directly increases the incident heat flux measurement. A detailed description of Schmidt-Boelter gauge

design/operation can be found in Carl Kidd's AEDC report<sup>4</sup>. The design and development of the three-dimensional Schmidt-Boelter gauge solid thermal model is presented next.

## SCHMIDT-BOELTER MODEL DESIGN AND DEVELOPMENT

A Schmidt-Boelter (S-B) gauge comprises four major components, including the cylindrical conductive gauge body, the non-conductive epoxy, the conductive rectangular wafer and the thermopile. Note that the gauge body and the wafer are typically composed of the same conductive material, usually copper and aluminum. A basic orientation of these parts is shown in Figure 3.

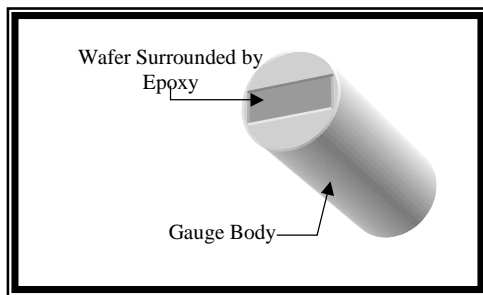


Figure 3: Basic Diagram of S-B Gauge

The gauge measures the temperature difference between the top and bottom surfaces of the wafer via the thermopile, outputting a signal proportional to the incident heat flux. The epoxy is exposed to the top surface of the gauge and completely encases the wafer and thermocouple wire. The idealizations incorporated by this 3-D model are shown in the figure below. Note that the thermocouple wire and beads are shown for explanation purposes only (Figure 4). Kidd analyzed the effects of the size and material of the thermocouple wire on heat transfer measurements, which show that wire having diameters less than 0.003 in (0.0762 mm) induce small errors<sup>4</sup>. Therefore, they are considered negligible for modeling construction because of their limited impact on the overall thermal environment.

material of the thermocouple wire on heat transfer measurements, which show that wire having diameters less than 0.003 in (0.0762 mm) induce small errors<sup>4</sup>. Therefore, they are considered negligible for modeling construction because of their limited impact on the overall thermal environment.

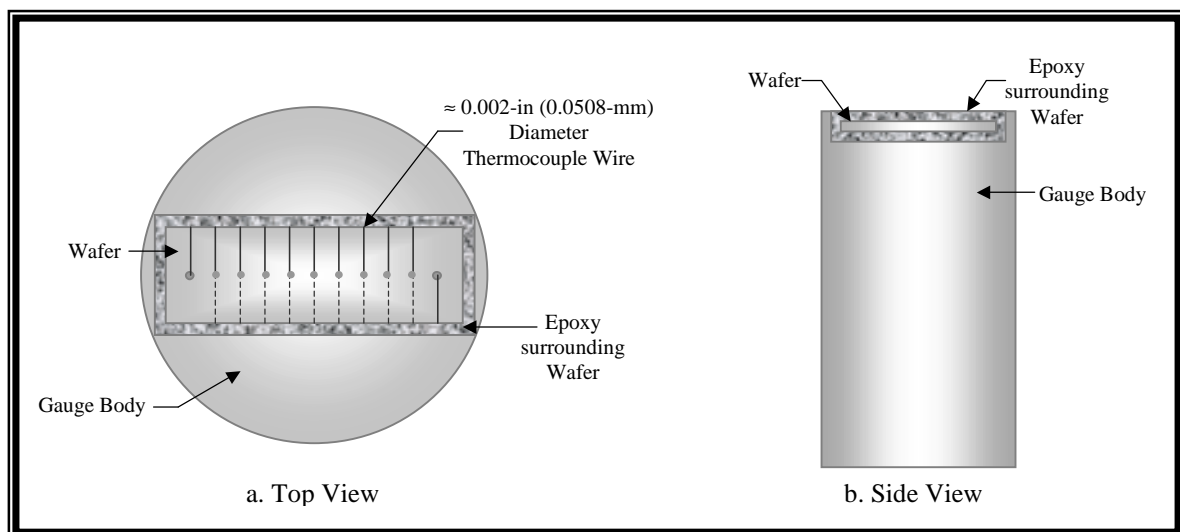


Figure 4: Idealization used for Modeling of the S-B Gauge

The software used to develop and analyze this model was SINDA/G 2.1, a finite-differencing thermal analyzer. Each node was manually generated in order to provide a customized model that

focuses on the temperature differences measured by the gauge. The 3-D Schmidt-Boelter gauge model consists of over 3600 nodes, the densest mesh being in the epoxy/wafer area. There is a high concentration of detail there because the effect on the epoxy/wafer is the focus of this radial heat transfer study. Less detail is needed for those nodes that are composed of the same material and are not located near the relative vicinity of the wafer.

## **AEROTHERMAL TESTING AT MARSHALL SPACE FLIGHT CENTER**

Both the CFD and the detailed gauge model calibrations will be achieved via testing of flat plates with thin skin calorimeters and copper and aluminum Schmidt-Boelter gauges. The thin skin calorimeters will indicate the actual heat flux, and the Schmidt-Boelter gauges will give readings that, when properly corrected by the calibrated models, will match the thin skin measurements. Test panels are shown in Figure 5, with a,b,and c already tested, and d awaiting testing in the Improved Hot Gas Facility (IGHF) at MSFC. Note that the diagrams are not to scale but the panels are 12 inches by 19 inches. There are two categories of test panels: with TPS and without TPS.

Three panels of different materials without TPS have already been tested. The materials include stainless steel, copper, and aluminum. Each includes one thin skin calorimeter of a material similar to the plate, and the stainless steel panel includes two more thin skin calorimeters on the same flow path line as the first to determine incident heat rate variations as a function of location along the major plate axis. Each of these plates also has two Schmidt-Boelter calorimeters of dissimilar materials, located as shown in Figure 5. The thin skin gauges are made of the same material as the plate and will give an accurate assessment of the incident convective heat flux, although the stainless steel thin skin gauge will give an accurate reading for a longer time period.

The fourth panel style will be stainless steel, partially covered by an ablative, low thermal conductivity material (also shown in Figure 5). The ablative material will most likely be BTA or cork, and will appear as rectangular strips on either side of a stainless steel strip centered and in the direction of flow. The ablative material will be approximately 0.125 in thick, and the stainless steel below the TPS will be machined out so the BTA is level with the center strip of stainless steel. Three thin skin calorimeters will be used, and will appear as in the stainless steel panel with no TPS. One copper and one aluminum S-B gauge will appear flush mounted with the TPS, each on a separate TPS strip.

Summarizing, four different panels have been designed. Three of these have already been fabricated and tested: 1) a copper panel with one copper S-B gauge, two aluminum S-B gauges, and a thin skin calorimeter; 2) an aluminum panel with one aluminum S-B gauge, two copper S-B gauges, and one thin skin calorimeter; and 3) a stainless steel panel with three thin skins, one copper S-B gauge, and one aluminum gauge. A fourth panel, stainless steel and partially covered with an ablative, has three thin skin gauges, one copper S-B gauge, and one aluminum S-B gauge. The copper gauges are Medtherm Schmidt-Boelters and the aluminum gauges are AEDC Schmidt-Boelters.

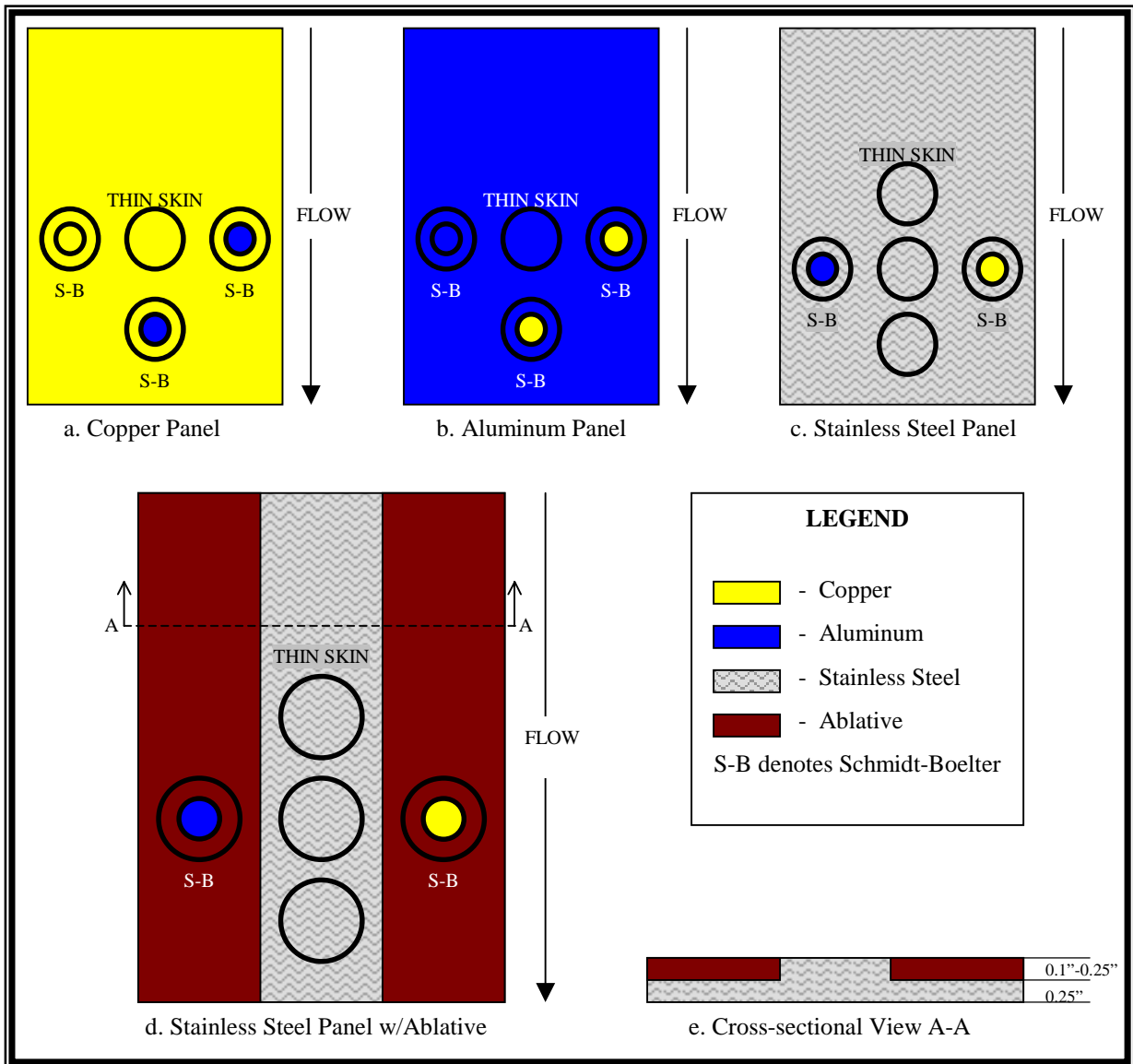


**Figure 5: Testing Panel Configuration**

The primary purpose of the study is determine dissimilar material effects, and the testing will be used for model calibration, that will build confidence for use of the models to correct in-flight data. In addition, the impact of gage/wafer orientation with respect to convective flow direction will also be studied in the testing program. The testing matrix shown below also includes a couple of radiant test points that will eliminated thermal boundary layer effects and allow focus on radial heat transfer effects. Thus, the calibration process will be as follows: Use the incident radiant testing to calibrate the solid thermal model, then use the convective testing to calibrate the coupled solid and CFD models.

**Table 1: Basic Testing Matrix**

Test # (by priority)	Panel	Angle	Approx. HR (Btu/ft <sup>2</sup> /s)	Comments	Time (s)
1	Stainless Steel Plate	0°	4.7	Baseline	20
2	Stainless Steel Plate	0°	4.7	Repeat Baseline	20
3	Aluminum Plate	0°	4.7	Baseline	20
4	Aluminum Plate	0°	4.7	Repeat Baseline	20
5	TPS/SS/Hypalon	0°	4.7	Baseline	20
6	TPS/SS/Hypalon	0°	4.7	Repeat Baseline	20
7	Copper Plate	0°	4.7	Baseline	20
8	Copper Plate	0°	4.7	Repeat Baseline	20
9	Stainless Steel Plate	0°	4.7	Baseline with Medtherm calorimeters rotated 120°	20
10	Stainless Steel Plate	0°	4.7	Repeat Baseline with Medtherm calorimeters rotated 120°	20
11	Stainless Steel Plate	0°	4.7	Baseline with Medtherm calorimeters rotated 240°	20
12	Stainless Steel Plate	0°	4.7	Repeat Baseline with Medtherm calorimeters rotated 240°	20
13	TPS/SS/Hypalon	TBD	8.0	Baseline	20
14	TPS/SS/Hypalon	TBD	8.0	Repeat Baseline	20
15	TPS/SS/Hypalon	0°	4.7	Baseline, radiant	20
16	TPS/SS/Hypalon	0°	4.7	Repeat Baseline, radiant	20
17	Aluminum Plate	0°	4.7	Baseline with Medtherm calorimeters rotated 120°	20
18	Aluminum Plate	0°	4.7	Repeat Baseline with Medtherm calorimeters rotated 120°	20
19	Aluminum Plate	0°	4.7	Baseline with Medtherm calorimeters rotated 240°	20
20	Aluminum Plate	0°	4.7	Repeat Baseline with Medtherm calorimeters rotated 240°	20
21	Copper Plate	0°	4.7	Baseline with Medtherm calorimeters rotated 120°	20
22	Copper Plate	0°	4.7	Repeat Baseline with Medtherm calorimeters rotated 120°	20
23	Copper Plate	0°	4.7	Baseline with Medtherm calorimeters rotated 240°	20
24	Copper Plate	0°	4.7	Repeat Baseline with Medtherm calorimeters rotated 240°	20

In addition to the usual IHGF measurements and the thin skin and S-B data, surface IR data will be important. Spot IR and surface plane IR data will be used to determine the surface temperature profile of the plate, focusing on the areas on and in the near vicinity of the S-B gauges. This information will be crucial in the model calibration efforts, especially for determining the boundary layer effects caused by the surface temperature differences between the panel and the S-B gauges. In addition, as explained later, the transient IR measurement also holds promise as a means of inferring the heat flux rate.

Finally, it will be important to understand the contact resistances between the S-B gauges and the surrounding material. The easiest way to establish this is by making the contact resistance as close to zero as possible using high conductivity thermal grease. In any event, determining the actual contact resistance will be a part of the calibration process.

## **POST-TEST MODEL ANALYSIS**

As mentioned previously, the primary goal of this study is to correct and better understand in-flight measurements of heat fluxes on launch vehicles. Test data from the aerothermal facility will be used to calibrate the analytical models. In addition, a sensitivity analysis can determine the impact of sensor orientation, wafer thickness, epoxy thickness, and contact conductances from the sensor to the surrounding material. In addition, during manufacturing, several deviances from production specifications can occur. For instance, the thermopile beads could be separated unevenly, they may not be centered, etc. The sensitivity analysis will investigate these types of variables and the effects they induce on the overall gauge measurement

## **ALTERNATE HEAT FLUX MEASUREMENTS**

The Schmidt-Boelter gauges use the one-dimensional Fourier's law to infer heat fluxes. Calorimeters exist that use the time rate of change of the calorimeter's bulk temperature to infer heat flux. Both of these depend on the gauge having a high conductivity and high specific heat, unlike most TPS, thus inducing the errors explained earlier. A potentially easier method of inferring heat flux is to directly measure the surface temperature of the TPS and infer the heat flux by calculating the incident heat flux required to produce the temperature rise. Embedded thermocouples have been used, but are also susceptible to sensor errors and wiring complications.

Infrared sensors and temperature sensitive paints are being investigated and characterized via IHGF testing as a potential means of measuring surface temperatures transient profiles, and will be compared with thin skin and Schmidt-Boelter gauges. IR data can be obtained either via a spot sensor or via an IR camera with a two dimensional surface temperature output. In flight, this would require an IR sensor or camera pointed at the surface of interest. This limits the configurations possible, but has the potential of providing accurate heat flux data.

Temperature sensitive paints, or paints that experience distinct color changes at discrete temperatures, also provide another method of measuring transient surface temperature profiles, and thus a heat flux measurement, but the resolution is very coarse, and this method could only be used for fairly smooth (nearly linear) transient temperature profiles. Ascent aeroheating profiles are good candidates, but re-entry profiles, in most cases, are not. The advantage to this method is that it can "piggyback" on launch vehicles that already provide video camera data with little to no extra cost.

## **CONCLUSIONS**

A three part program has been assembled that will produce a calibrated technique to correct material dissimilarity induced errors for in-flight Schmidt-Boelter heat flux measurements on launch vehicles. In general, the need for such corrections is greatest for aerothermal heating measurements. Two coupled models have been developed, one correcting boundary layer effects stemming from near step changes in the temperature from the surrounding material to the gauge, and the other accounting for radial heating errors. Testing in an aerothermal facility will provide

the calibration. While this approach is more crucial to aerothermal heating measurements, the radial conduction effects model can also be applied to radiative measurement corrections, such as for plume radiation. These efforts are unique because they use CFD for boundary layer corrections and because they couple and calibrate the boundary layer effect model and the radial conduction model. In addition, alternate heat flux measurement methods involving IR measurements and temperature sensitive paints will be explored and characterized. While current uncorrected data and collection methods provide conservative factors of safety, there are potential benefits attainable from reduced conservatism via lower TPS mass and reduced TPS application requirements.

## ACKNOWLEDGEMENTS

The author(s) wish to acknowledge the help of the people at the MSFC Improved Hot Gas Facility, who have entered into a cooperative effort with us to obtain the necessary calibration data. Their assistance in fabricating the test panels and interfacing with heat flux gauge manufacturers and calibrators has been invaluable.

## REFERENCES

1. Reynolds, W. C., Kays, W. M., and Kline, S. J., "Heat Transfer in the Turbulent Incompressible Boundary Layer, II – Step Wall-Temperature Distribution," in *NASA Memorandum*, Washington, NASA, 1958, pp. 1-3.
2. Rubesin, Morris W., "The Effect of an Arbitrary Surface-Temperature Variation along a Flat Plate on the Convective Heat Transfer in an Incompressible Turbulent Boundary Layer," in *NACA Technical Note 2345*, Moffett Field, CA, NACA, 1951, pp. 1-3, 24.
3. Kidd, C. T., "A Durable, Intermediate Temperature, Direct Reading Heat Flux Transducer for Measurements in Continuous Wind Tunnels," in *AEDC-TR-81-19*, Arnold AFS, TN, AEDC, 1981, pp. 7-15.
4. Kidd, C. T., "Thin-Skin Technique Heat-Transfer Measurement Errors Due to Heat Conduction into Thermocouple Wires," *ISA Transactions* **24**, no. 2, 1985, pp. 1-9.

## CONTACT

Dr. Reinarts can be reached at the following e-mail address : [Thomas.reinarts-1@ksc.nasa.gov](mailto:Thomas.reinarts-1@ksc.nasa.gov).

## NOMENCLATURE, ACRONYMS, ABBREVIATIONS

M	Mach Number
Re	Reynolds Number
$T_{\infty}$	Free Stream Temperature

$T_{w1,w2}$	Wall Temperature
L	Running Length to Heat Flux Gauge
R	Radius of Heat Flux Gauge
W	$L+2R$
$q''$	Incident Heat Flux
$\delta T$	Differential Temperature
$\delta x$	Differential Length
TPS	Thermal Protection System
KSC	Kennedy Space Center
MSFC	Marshall Space Flight Center
IHGF	Improved Hot Gas Facility
AEDC	Arnold Engineering Development Center
S-B	Schmidt-Boelter
CFD	Computational Fluid Dynamics
$k_f$	Fluid thermal conductivity
$\nabla T_{f0}$	Temperature gradient of the fluid at the fluid wall interface